DOI: 10.1002/cphc.200900974

Molecular Wires in Single-Molecule Junctions: Charge Transport and Vibrational Excitations

Stefan Ballmann,[a, b] Wolfgang Hieringer,[b] Daniel Secker,[a] Qinglin Zheng,[d] John A. Gladysz,[c, d] Andreas Görling,[b] and Heiko B. Weber*[a]

We investigate the effect of vibrations on the electronic transport through single-molecule junctions, using the mechanically controlled break junction technique. The molecules under investigation are oligoyne chains with appropriate end groups, which represent both an ideally linear electrical wire and an ideal molecular vibrating string. Vibronic features can be detected as satellites to the electronic transitions, which are assigned to longitudinal modes of the string by comparison with density functional theory data.

1. Introduction

Electrical transport through molecules is a new and interesting field in physics, combining the physics of molecules with the concept of quantum transport. In molecules, the importance of vibrations for electronic processes is well known for optical excitations and for single-charge transfer processes, but the steady-state currents flowing in a molecular junction require new considerations. Still, similar to vibronic sidebands in optical spectroscopy, side structures to the electronic transitions are also expected for electrical characteristics.[1,2]

Experimental investigations on molecular junctions were carried out using the mechanically controlled break junction (MCBJ) technique. This method allows the formation of stable symmetric contacts while the molecule is covalently bound to gold electrodes with adjustable distance. Herein, we report on the design of the underlying molecules and experimental as well as theoretical investigations of vibrational traces in the electronic characteristics of a single-molecule junction. The molecule of choice was designed in the spirit of forming a vibrating molecular wire as an analog to an ideal string. We chose an oligoyne wire as a string-forming unit (see Figure 1 and refs. [3,4] for synthesis and standard characterization). Other oligoyne compounds have recently been investigated with a scanning tunneling microscopy (STM) setup.[5] Oligoynes are fully conjugated, essentially linear, and include no aryl structures as in nearly every molecular wire investigated before in conductance experiments. The eight-atom carbon chain characteristic of a tetrayne (without any side groups) is one of the simplest molecular wires that can be conceptualized. It is fixed in between two platinum(II) atoms, bearing the usual thiol end groups, which are the best-established linker units for forming metal–molecule–metal junctions.[6] This end group combination provides a fixed end to the conjugated wire, both electronically as well as for vibrational standing waves. Acetyl protecting groups at the utmost ends are well known as a suitable protecting unit that splits off upon contact with the gold electrode. The purpose of the phosphine ligands at the platinum atoms is to stabilize the molecule chemically.

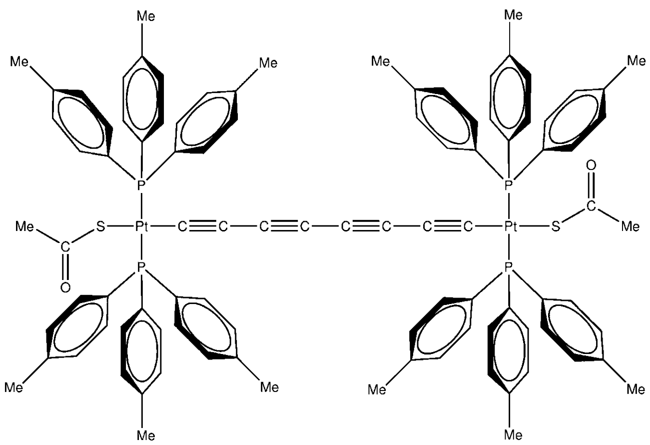

Figure 1. Structure of the molecule under investigation. The conjugated carbon chain consists of eight sp hybridized atoms and spans two heavy platinum atoms that are protected by bulky ligands. The thiol-acetyl functional group is cleaved by gold surfaces.

For the experiment carried out here, they are helpful in keeping a sufficient spacing between possible neighbor molecules and thus for protecting the molecular wires against uncontrolled background charges or environmental disorder.

[a] S. Ballmann, Dr. D. Secker, Prof. H. B. Weber
Chair of Applied Physics, University of Erlangen-Nürnberg
Staudtstr. 7/Bau A3, 91058 Erlangen (Germany)
Fax: (+49) 9131-8528423
E-mail: heiko.weber@physik.uni-erlangen.de

[b] S. Ballmann, Dr. W. Hieringer, Prof. A. Görling
Chair of Theoretical Chemistry
University of Erlangen-Nürnberg
Egerlandstr. 3, 91058 Erlangen (Germany)

[c] Prof. J. A. Gladysz
Department of Chemistry, Texas A&M University
PO Box 30012, College Station, Texas 77843-3012 (USA)

[d] Q. Zheng, Prof. J. A. Gladysz
Institute of Organic Chemistry, University of Erlangen-Nürnberg
Henkestr. 42, 91054 Erlangen (Germany)

Supporting information for this article is available on the WWW under http://dx.doi.org/10.1002/cphc.200900974.

The simplest picture of charge transport across conjugated molecules is resonant tunneling, which predicts that charge can flow above a certain threshold voltage, when the first molecular orbital is in the energy window defined by the chemical potential of the leads and the applied voltage. These electronic transitions, which are observable as peaks in the differential conductance d*I*/d*V*, are accompanied by vibronic sidepeaks,[7,8] separated from the electronic peak by the vibrational energies $2\hbar\omega$ of the first or higher harmonics in case of symmetric coupling and equal voltage drop at both sides of the contact.[9–11] In ungated single-molecule junctions (mechanically controlled break junctions), the electronic threshold often lies at voltages larger than ± 0.5 V, which allows complicated processes to be triggered as soon as current flows. The observation is typically a broad peak, where vibronic sidebands are smeared out. In gated devices (which so far have rigid electrodes and typically not a relaxed metal-molecule-metal junctions), this threshold can be lowered towards zero volts, and vibrational lines can be resolved. If the charge degeneracy is lifted and the current threshold rises beyond a few tens of mV, the sidebands are blurred, and a broad electronic/vibronic transition is observed.[2]

To classify the individual vibrational modes we performed frequency analyses by means of density functional theory (DFT) based calculations.[12,13] Herein, we present the results of the DFT calculations in comparison with experimental data.

2. Results and Discussion

2.1. DFT Calculations

Before discussing the experimental results, we briefly describe our standard density functional calculations on the geometries and vibrational spectra of a model junction consisting of the oligoyne with simplified phosphine ligands and the sulfur atoms attached to gold clusters at both ends. The goal was to understand the vibrational properties of the molecules and the junction and to compute the energies of the vibrational eigenmodes. There are $3N-6$ normal modes of the N-atom system, many of them being irrelevant for charge transport. The main focus shall be on the four energetically lowest-lying longitudinal modes of the carbon chain, which were resolved in the experiment (see Figure 2).

The computations include various phosphine ligands [P(p-tol)$_3$, PMe$_3$, PH$_3$], specific contact realizations (on-top position S–Au, bridge position S–Au$_2$, hollow position S–Au$_3$) as well as an approximate simulation of mechanical stress by pulling and pushing the carbon chain (see Supporting Information, Figure S1). We find that different contact geometries have significant influence on the orbital eigenvalues of the underlying system similar to the observations made in ref. [14]. However, neither the different types of phosphine ligands nor the various contact realizations show relevant impact on the vibrational frequencies of the chain. This result justifies a direct interpretation of the measurements since the specific contact geometry of the sulfur atoms and the gold leads is an uncontrolled parameter in the experiment. As a consequence, spontaneous reconfigurations of the contacts should not affect vibronic signatures of the chain in the current–voltage characteristics of single-molecule junctions.

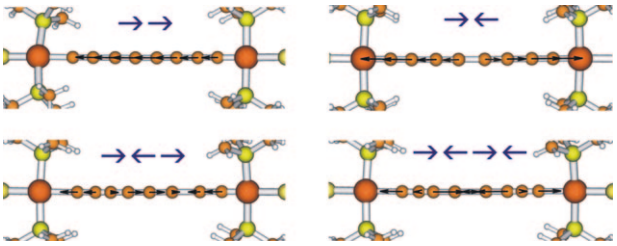

Figure 2. Displacement of the carbon atoms in the chain for the four energetically lowest-lying longitudinal modes.

Table 1 shows the vibrational energies for the fundamental longitudinal excitation (38 meV) and its higher harmonics as calculated using DFT. The values for the higher harmonics follow roughly the simple rule of integer multiples of the fundamental oscillation energy, which is well known for a homogenous elastic medium. It should be noted that the vibrational energy of the fundamental transversal stringlike excitation lies around 6 meV. This energy scale cannot be observed in the experiments.

Table 1. Comparison of the experimentally (MCBJ) and theoretically (DFT) observed vibrational energies. The first and third harmonic in the experimental data are averaged in energy as they occur in both d*I*/d*V* curves.

method	vibrational energy E_{vib} [meV]			
	→→	→←	→←→	→←→←
DFT	38	80	127	171
MCBJ	36	89	124	167
MCBJ ($d=-2$ Å)	46	92	129	167

For further comparison with experimental data, we considered small distance variations of the junction. We have simulated strain and compressive strain by parametrically varying the distance of the two sulfur atoms at both ends of the molecule and allowing for a geometry relaxation within this constraint. An increase in this S···S distance, that is, an elongation of the molecule beyond its equilibrium length, causes a weakening of the carbon bonds. Consequently, the total energy rises quadratically as the string is stretched (see Figure 3 a), while the vibrational energies of the longitudinal modes decrease approximately linearly (see Figure 3 b). Compression results in a bending of the chain in a way that the bond angles but not the bond lengths between the carbon atoms are altered. Therefore, the total energy as well as the vibrational energies of the longitudinal modes are only increased marginally.

2.2. Experimental Data

The interpretation of the *I*–*V* characteristics of single molecules is challenging since the resonant tunneling model is inappropriate at high bias voltages. At the onset of charge transport,

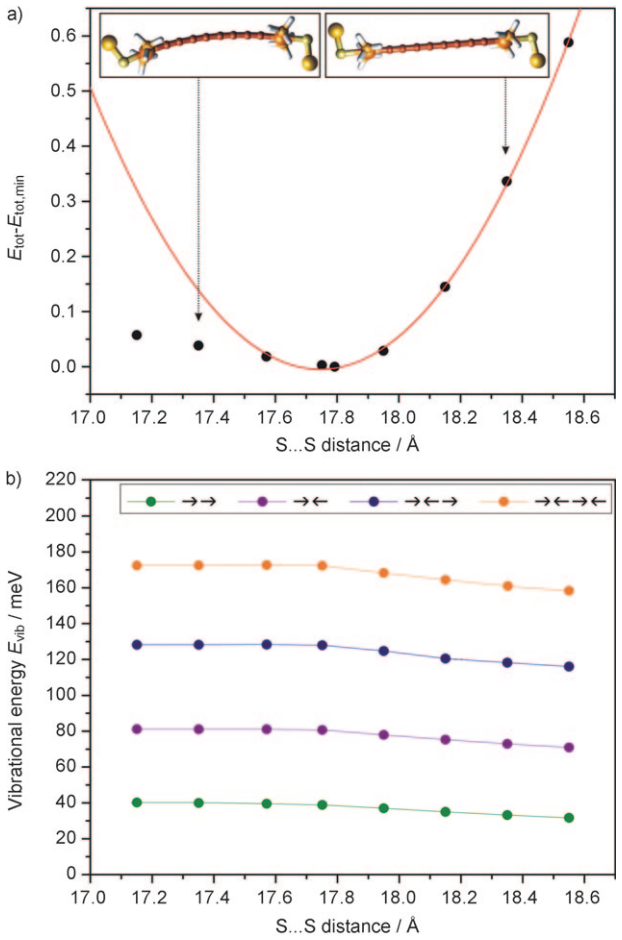

Figure 3. Plot of the calculated total energy and vibrational energies of the longitudinal modes versus the distance between the sulfur atoms at the two ends of the molecule.

peaks in d*I*/d*V* experience a broadening of about 100 mV. Their origin can be ascribed to ensemble averaging, unresolved excitations, charge reconfigurations and structural fluctuations of the molecule.[15] As a result, the resolution of vibrational excitations is only achieved in a small number of sufficiently stable junctions, in which by chance other instabilities were frozen out. The yield in generation of long-term stable junctions may be limited by the rather bulky ligand structure of the molecule obscuring the linkage groups. According to our experience with many thiol-acetyl capped molecular rods, the observed stability can be assigned to covalent sulfur-gold bonds.

Herein, we report on such a stable junction where we measured the *I*–*V* characteristics of the covalently bond molecule by sweeping a dc voltage from −1.5 to 1.5 V at a temperature of 75 K (see Figure 4a). The green curves are the average of five *I*–*V* curves at a fixed electrode separation, both for the up and down sweeps, while the blue curves are numerical derivatives of the latter, smoothed according to the Savitzky–Golay method. A detailed view of the average d*I*/d*V* characteristics in Figure 4b,c clearly shows a sequence of peaks that were fitted by Lorentzian functions. Similar features occur in both the up- and down-sweep of the bias voltage, which show a slight shift of 24 mV. Besides this "hysteresis", which occurs in many single-molecule junctions, we observe a symmetric onset of the current at ±0.8 V. We attribute the first peak to the onset of charge transport through an electronic level and the satellite peaks to vibrational excitations of the molecule, whereas the relative distances of the satellites with respect to the electronic peak are twice the vibrational energies E_{vib} of the excitations since the bias voltage should drop equally at both ends of the molecule for such highly symmetric *I*–*V* characteristics.

According to the geometry of the molecule, stringlike excitations can be expected to play a prominent role, rather than side group vibrations. In comparing the experimental data to our calculations, we find an excellent agreement for the excita-

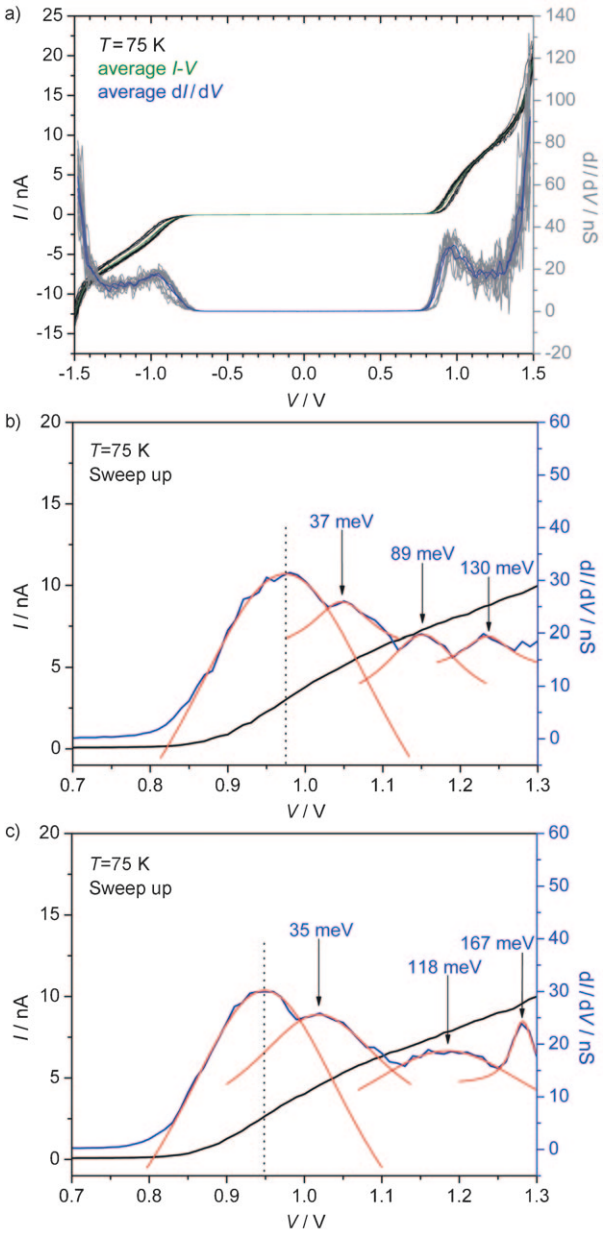

Figure 4. Plot of the current *I* (a) and enlarged details of the differential conductance d*I*/d*V* for up and down sweep (b,c) versus the bias voltage *V*. The d*I*/d*V* curves are averaged and smoothed according to the Savitzky–Golay method.

tions of longitudinal modes since the corresponding energies match the DFT-based predictions perfectly (see Table 1).

For further clarification we investigated the behavior of the excitations under small distance variations of the junction. A reduction of the electrode spacing by about $d = 2$ Å leads to a shift of the peaks in d*I*/d*V*, but the vibrational energies derived from peak distances are nearly unchanged, with only a small increase. This behavior could be ascribed to a reconfiguration of the contact geometry or to a marginal bend of the carbon chain. Both scenarios keep—according to our theoretical calculations—the bond lengths constant and therefore the vibrational energies remain unchanged. Also a compression of the molecule leads to a marginal increase of the vibrational energies of longitudinal modes. In either case the DFT-based predictions fit well to our experimental results and support the observation of longitudinal excitations respectively.

However it remains an open question as to why particular longitudinal modes are detected. In vibrational tunneling spectroscopy, no selection rules based on symmetry are valid. In the inelastic tunneling (IETS) regime, perturbative *propensity rules* instead of strict selection rules are used,[16–18] but they can not easily be transferred to the resonant tunneling regime.

We propose a picture which considers the fundamental process of charge flow: one electron tunnels off the molecule towards the drain electrode, leaving a charged cationic state behind, which is subsequently filled by an electron tunneling from the source electrode onto the molecule. The charged intermediate state will relax into a different geometrical configuration. This viewpoint disregards that tunneling times and relaxation times are not clearly separated in our experiment, but might nevertheless serve as an intuitive picture.

In our type of molecule, the charge will be located in the conjugated wire, and a missing electron will weaken bonds and relax the linear conjugated system. Hence, charging and uncharging will result in a variation of the length of the molecule (at least if no fixed ends are considered). This qualitative argument may give a hint why the electronic transport couples most efficiently to the *longitudinal* modes of vibration. Further evidence for this conjecture comes from the theoretical analysis of model systems of different sizes (see Supporting Information, Figure S2). The highest occupied molecular orbital (HOMO) in all considered systems is a bonding π-type orbital which is predominantly located on the carbon chain and contributes to the carbon–carbon triple bonds (see Figure 5). Removal of an electron from this orbital weakens the carbon–carbon triple bonds and thus is expected to change the bonding distances in the carbon chain. A sudden charging of the molecule is therefore expected to result in an excitation of longitudinal vibrational modes. To quantify this effect, we have optimized the geometry of the cationic molecule and projected the change in geometry compared to the uncharged molecule on the vibrational modes of the uncharged molecule (see Section 4 for further details). This analysis reveals that within the energy range of the relevant vibrations, predominantly longitudinal modes are excited upon charging of the model system. Furthermore, the longitudinal modes calculated at energies of 80 meV and 171 meV (see Table 1), respectively, which have been assigned to the experimental signatures at 89 and 167 meV, show an increased projection coefficient, thus providing further support to our assignment. The other two modes do not show a significant coefficient, which may be attributed to the simplified model systems used in the analysis. Similar results are obtained if the changes of the geometries of the neutral and charged molecules are projected on the vibrational modes of the cationic or anionic molecules.

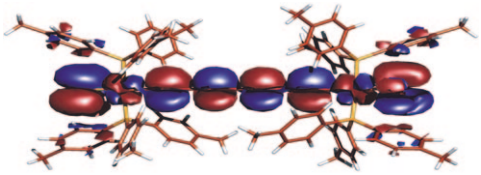

Figure 5. Contour plot of the molecule's highest occupied molecular orbital (HOMO) as calculated with DFT. Each of the sulfur atoms is bound to one gold atom at the utmost ends.

For negative bias voltages, the peaks in d*I*/d*V* show equal behavior but are less pronounced. Further vibrational modes are likely to be excited but might not be resolved properly. This could cause an enhancement of the peak broadening in the vicinity of longitudinal signatures. From the electronic structure and vibrational spectra of the calculated model systems, we presently cannot fully exclude that at least one molecular orbital of the molecule might also give rise to a satellite peak in the differential conductance. However by comparison of the underlying peak widths, the scaling of the vibrational energies and the drastic increase in current beyond 1.3 V, we have strong evidence that all the satellites in d*I*/d*V* can be attributed uniquely to vibrational signatures.

3. Conclusions

It has been shown that charge transport through single molecules is accompanied by internal molecular vibrations that can be accessible by means of the mechanically controlled break junction technique. The molecule under investigation was chosen as a rodlike oligoyne in order to establish well-defined vibrational modes for further investigations of inelastic processes. The experimental data show strong indications for the observation of vibrational features as peaks in d*I*/d*V* at a temperature of 75 K. The measured vibrational energies are in excellent agreement with density functional calculations for the four energetically lowest-lying longitudinal modes of the carbon chain. Some unresolved issues concerning peak widths and resolution of the excitations have been discussed.

The results should be further supported and verified by changing the molecules' chain length synthetically so that the vibrational frequencies are altered analogously. Work is underway in this direction.

Methods

Theoretical investigations were performed based on density functional theory (DFT) using the TURBOMOLE package (version 5.7).[19] The exchange-correlation functional due to Becke and Perdew

(BP86)[20,21] was used in combination with the standard TZVP (triple-zeta valence plus polarization)[22] Gaussian basis sets from the TURBOMOLE basis set library. The platinum and gold atoms were treated using effective core potentials. The resolution of the identity (RI) technique was used throughout.[23] The BP86 functional is known to predict useful vibrational frequencies for compounds involving transition metal atoms.[24,25] The molecule and gold clusters were first optimized separately and then combined in a model junction. Each fully optimized structure—given by an arrangement of gold clusters representing the leads and the covalently bound oligoyne—was then subjected to a frequency analysis. The vibrational normal modes were visualized with the Molden program.[26] To analyze which of the vibrational modes are likely to be excited during the electron transport through the molecule, the change in molecular geometry of a model system upon charging was calculated and this geometry change was projected on the vibrational normal modes of the uncharged molecule as well as on the vibrational modes of the charged molecule. The projection was done by solving the linear system $Q\underline{x} = \Delta\underline{g}$ for $\underline{x}$, where Q is a matrix with the normal modes in terms of atomic displacements in the columns and $\Delta\underline{g}$ is the vector containing the differences in atomic positions between the uncharged and charged molecules. Large entries in the coefficient vector $\underline{x}$ thus identify those normal modes which are related to the change in geometry when charging the system and which may thus be excited upon charging of the molecule.

Investigations on charge transport were performed utilizing the mechanically controlled break junction (MCBJ) technique. Structured by electron-beam lithography, a 100 nm thick gold bridge with a lateral constriction and electrical contacts were evaporated on a flexible isolating substrate (200 μm phosphorous bronze coated with 4 μm polyimide). A part of the polyimide was removed by reactive ion etching so that the constriction becomes freestanding (see Supporting Information, Figure S3). The sample was mounted in a three-point bending mechanism which is driven by a linear motor and a differential thread. An applied mechanical force causes an elongation of the gold bridge until it finally breaks at its narrowest point. The hereby created atomically sharp tips serve as separated electrodes which have proven to be ideal for controlled immobilization of single molecules. The experimental setup allowed for formations of long-term stable contacts and manipulations of the contact configuration upon variation of the electrodes' spacing with an accuracy of the order of one angstrom under ultrahigh-vacuum conditions in a temperature range from 8 to 300 K.[27–30] A detailed discussion of the mechanism and the fabrication of the substrates has been published elsewhere.[31] The molecules are applied in tetrahydrofuran solution onto an open junction. After evaporation of the solvent in a dry nitrogen flow, the vacuum chamber is evacuated. As the gold electrodes are approached, a sudden lock-in behavior to a plateau of nearly constant conductance is indicative for a molecule bridging the gap between the tips (see Supporting Information, Figure S4). At this point, the substrate is cooled down by liquid helium and *I/V* characteristics of single molecules can be recorded by a source–measure unit.

Acknowledgements

This work was carried out in the framework of the Cluster of Excellence "Engineering of Advanced Materials" and the Interdisciplinary Center for Molecular Materials (ICMM) at the Friedrich-Alexander-Universität Erlangen-Nürnberg. Support of the National Science Foundation (CHE-0719267) is gratefully acknowledged by J.A.G. We furthermore thank Michael Thoss, Rainer Härtle and Oscar Rubio-Pons for helpful discussions.

Keywords: density functional calculations · electron transport · mechanically controlled break junction · molecular electronics · oligoyne

[1] D. Djukic, K. S. Thygesen, C. Untiedt, R. H. M. Smit, K. W. Jacobsen, J. M. van Ruitenbeek, *Phys. Rev. B* **2005**, *71*, 161402.
[2] E. A. Osorio, K. O'Neill, N. Stuhr-Hansen, O. F. Nielsen, T. Bjørnholm, H. S. J. van der Zant, *Adv. Mater.* **2007**, *19*, 281.
[3] Q. Zheng, J. C. Bohling, T. B. Peters, A. C. Frisch, F. Hampel, J. A. Gladysz, *Chem. Eur. J.* **2006**, *12*, 6486.
[4] a) W. Mohr, J. Stahl, F. Hampel, J. A. Gladysz, *Chem. Eur. J.* **2003**, *9*, 3324; b) W. Mohr, J. Stahl, F. Hampel, J. A. Gladysz, *Inorg. Chem.* **2001**, *40*, 3263.
[5] C. Wang, A. S. Batsanov, M. R. Bryce, S. Martín, R. J. Nichols, S. J. Higgins, V. M. García-Suárez, C. J. Lambert, *J. Am. Chem. Soc.* **2009**, *131*, 15647.
[6] a) J. M. Tour, L. Jones II, D. L. Pearson, J. J. S. Lamba, T. P. Burgin, G. M. Whitesides, D. L. Allara, A. N. Parikh, S. V. Atre, *J. Am. Chem. Soc.* **1995**, *117*, 9529; b) J. M. Tour, *Acc. Chem. Res.* **2000**, *33*, 791.
[7] W. Wang, T. Lee, I. Kretzschmar, M. A. Reed, *Nano Lett.* **2004**, *4*, 643.
[8] B. C. Stipe, M. A. Rezaei, W. Ho, *Science* **1998**, *280*, 1732.
[9] E. G. Emberly, G. Kirczenow, *Phys. Rev. B* **2000**, *61*, 5740.
[10] J. G. Kushmerick, J. Lazorcik, C. H. Patterson, R. Shashidhar, D. S. Seferos, G. C. Bazan, *Nano Lett.* **2004**, *4*, 639.
[11] M. Galperin, M. A. Ratner, A. Nitzan, *J. Chem. Phys.* **2004**, *121*, 11965.
[12] P. Hohenberg, W. Kohn, *Phys. Rev. B* **1964**, *136*, 864.
[13] W. Kohn, L. J. Sham, *Phys. Rev. A* **1965**, *140*, 1133.
[14] H. B. Weber, J. Reichert, F. Weigend, R. Ochs, D. Beckmann, M. Mayor, R. Ahlrichs, H. von Löhneysen, *Chem. Phys.* **2002**, *281*, 113.
[15] D. Secker, H. B. Weber, *Phys. Status Solidi B* **2007**, *244*, 4176.
[16] A. Troisi, M. A. Ratner, *Nano Lett.* **2006**, *6*, 1784.
[17] A. Gagliardi, G. C. Solomon, A. Pecchia, Th. Frauenheim, A. Di Carlo, N. S. Hush, J. R. Reimers, *Phys. Rev. B* **2007**, *75*, 174306.
[18] N. Lorente, M. Persson, L. J. Lauhon, W. Ho, *Phys. Rev. Lett.* **2001**, *86*, 2593.
[19] R. Ahlrichs, M. Bär, M. Häser, H. Horn, C. Kölmel, *Chem. Phys. Lett.* **1989**, *162*, 165.
[20] A. D. Becke, *Phys. Rev. A* **1988**, *38*, 3098.
[21] J. P. Perdew, *Phys. Rev. B* **1986**, *33*, 8822.
[22] A. Schäfer, C. Huber, R. Ahlrichs, *J. Chem. Phys.* **1994**, *100*, 5829.
[23] a) K. Eichkorn, O. Treutler, H. Öhm, M. Häser, R. Ahlrichs, *Chem. Phys. Lett.* **1995**, *240*, 283; b) K. Eichkorn, F. Weigend, O. Treutler, R. Ahlrichs, *Theor. Chem. Acc.* **1997**, *97*, 119.
[24] J. Neugebauer, B. A. Hess, *J. Chem. Phys.* **2003**, *118*, 7215.
[25] A. P. Scott, L. Radom, *J. Phys. Chem.* **1996**, *100*, 16502.
[26] G. Schaftenaar, J. H. Noordik, *J. Comput.-Aided Mol. Des.* **2000**, *14*, 123.
[27] C. J. Muller, J. M. van Ruitenbeek, L. J. de Jongh, *Phys. Rev. Lett.* **1992**, *69*, 140.
[28] M. A. Reed, C. Zhou, C. J. Muller, T. P. Burgin, J. M. Tour, *Science* **1997**, *278*, 252.
[29] J. Reichert, R. Ochs, D. Beckmann, H. B. Weber, M. Mayor, H. von Löhneysen, *Phys. Rev. Lett.* **2002**, *88*, 176804.
[30] H. B. Weber, J. Reichert, R. Ochs, D. Beckmann, M. Mayor, H. von Löhneysen, *Phys. E* **2003**, *18*, 231.
[31] E. Lörtscher, H. B. Weber, H. Riel, *Phys. Rev. Lett.* **2007**, *98*, 176807.

Received: December 10, 2009
Revised: February 19, 2010
Published online on June 2, 2010

